

This is the preprint version (before review) of :

Selecting tandem partners for silicon solar cells

Zhengshan (Jason) Yu, Mehdi Leilaouioun & Zachary Holman, Nature Energy 1, Article number: 16137 (2016).

The published version (doi:10.1038/nenergy.2016.137) is available at:

<http://www.nature.com/articles/nenergy2016137>

Learning to play with others: Silicon goes tandem

Zhengshan (Jason) Yu, Mohammadmehdi Leilaeioun, Zachary Holman

Arizona State University

Photovoltaic (PV) module efficiency is a key driver of solar electricity cost reduction^{1,2}, particularly in markets that have high area-dependent balance-of-system costs, like the residential PV market. The efficiencies of commercial PV modules—and, naturally, their constituent cells—have risen dramatically in response: Multi-crystalline silicon modules, which make up roughly 60% of the PV market, have jumped from 15.5% efficiency in 2010 to 19.2% efficiency in 2015³. Additionally, companies such as Panasonic, SunPower, and Kaneka have recently reported large-area monocrystalline silicon cells with efficiencies exceeding 25%⁴. These are nearing the 29.4% maximum possible efficiency for a silicon cell⁵ and may soon reach the oft-claimed 26% practical efficiency limit⁶. To push cell and module efficiencies still higher, the PV industry will need to transition to the only device structure that has successfully surpassed the (single-junction) detailed-balance limit: multi-junctions.

Fortunately, silicon, the dominant PV technology, has many of the characteristics desired of a bottom cell in a tandem. It is abundant, efficient, and inexpensive (70–170 \$/m² for modules), it has a near-ideal bandgap (1.12 eV) for maximum tandem efficiency⁷, and there are 60 GW of existing production capacity⁸. III-V multi-junction cells, which have achieved 46% efficiency, would seem a natural example to follow in the development of efficient silicon-based tandems. However, III-V cells leverage epitaxial growth to access a wide range of bandgaps, and the same approach does not easily translate to silicon because of its unique lattice constant and few alloying partners. The challenge, then, is to identify and develop an efficient top cell—which likely will not be epitaxially grown on silicon and may be polycrystalline—as well as a suitable configuration for coupling it with a silicon bottom cell.

State-of-the-art

Figure 1a summarizes the highest one-sun efficiencies achieved to date for tandems with silicon bottom cells and a range of both top cells and coupling configurations. III-V/silicon tandems have the longest development history and presently top the efficiency chart: A 29.8%-efficient tandem was demonstrated in 2016 by mechanically stacking a 1.8-eV GaInP cell on a silicon heterojunction cell⁹. Mature thin-film PV technologies such as CdTe, CIGS, and amorphous silicon are absent from the chart, as no efficient,

wide-bandgap cells have been fabricated. This is due at least in part to a history of viewing crystalline silicon as a competitor in the single-junction PV market and not as a tandem partner in need of a top cell. One 1.8-eV CdZnTe top cell epitaxially grown on silicon has been reported¹⁰, however, and similar, polycrystalline cells could in principle be deposited with the existing CdTe manufacturing capacity. All other tandems in Figure 1a utilize lead halide perovskite cells, which, with their wide and tunable bandgaps and rapidly increasing efficiency, have recently emerged as another popular top-cell choice. A maximum efficiency of 28.0% has been measured using physically separated silicon and perovskite cells coupled with a beam splitter¹¹; and several groups have reported tandem efficiencies of around 20% with geometries more compatible with flat-plate PV modules^{12,13}.

Figure 1a hints that, among record laboratory cells, four terminals are better than two. (Compare, for example, the two tandems made by EPFL with the same sub-cells.) This can be understood by examining the common coupling configurations illustrated in Figure 1b. In two-terminal configurations, the sub-cells are connected in series and their currents must be matched at their maximum power points to avoid power loss. In four-terminal configurations, by contrast, the power output of each sub-cell is measured independently. Removing the current-matching constraint means that precise control of the top-cell bandgap and thickness, front-surface reflection, and parasitic absorption in supporting layers is no longer required. Moreover, four-terminal tandems in the field are expected to have up to 15% higher energy yield than equivalent-efficiency two-terminal tandems because they are insensitive to current mismatch resulting from spectrum variation¹⁴. Four-terminal configurations also allow for two monocrystalline sub-cells to be paired without epitaxial growth and without necessitating the clean, mirror polished surfaces demanded by bonding, or for sub-cells that have incompatible processing temperatures or chemistries to be paired. Despite these apparent advantages, no four-terminal tandem has been commercialized; III-V concentrator and space multi-junction cells, as well as thin-film silicon tandems, are monolithic two-terminal devices. Commercial four-terminal tandems are expected to have higher module and balance-of-systems costs than their two-terminal cousins, and the jury is out as to whether the value of increased efficiency in future markets will outweigh the cost of increased complexity.

Efficiency limits

What efficiency might a silicon-based tandem be expected to reach? A top-down approach to this question begins by calculating the limiting efficiency, which others have done using a detailed-balance model that considers only radiative recombination¹⁵. A more accurate treatment of the indirect-bandgap

silicon bottom cell must also include Auger recombination and incomplete photon absorption⁵, however, and thus Figure 1c shows the limiting efficiency of a tandem comprised of a radiative-recombination-limited top cell of variable bandgap and an Auger-recombination-limited silicon bottom cell with Lambertian light trapping. For a two-terminal configuration, a top cell with a bandgap of approximately 1.7 eV is best, and the tandem has a limiting efficiency of 43% under one-sun illumination. For the reasons discussed above, four-terminal configurations are less sensitive to the bandgap of the top cell but also have a peak efficiency near 1.7 eV. Were tandem cells to reach the same level of maturity as monocrystalline single-junction PV technologies such as silicon and GaAs, which have achieved cell efficiencies that are more than 85% of their respective limits, they would operate with over 36% efficiency.

Spectral efficiency: A new tool

A different, bottom-up approach to assess the potential of silicon-based tandems is to ask: What would happen if two *existing* sub-cells were paired? Which cells should one choose and what efficiency is possible? The limiting efficiency calculations used to generate Figure 1c, which consider hypothetical, ideal cells, are no help here. Instead, we turn to a little-known concept called “spectral efficiency”^{16,17}, $\eta(\lambda)$, defined as:

$$\eta(\lambda) = \frac{V_{oc} \cdot FF \cdot J_{sc}(\lambda)}{I(\lambda)}, \quad (1)$$

with V_{oc} the open-circuit voltage, FF the fill factor, $I(\lambda)$ the spectral irradiance (in $\text{Wm}^{-2}\text{nm}^{-1}$), and $J_{sc}(\lambda)$ the short-circuit current density at each wavelength:

$$J_{sc}(\lambda) = q \frac{\lambda}{hc} EQE(\lambda) \cdot I(\lambda). \quad (2)$$

Equation 1 looks like the usual definition of PV cell efficiency, but it is spectrally resolved. Spectral efficiency depicts efficiency at each wavelength and—in analogy with external quantum efficiency (EQE) and J_{sc} —its spectrum-weighted integral is cell efficiency. To calculate spectral efficiency, one needs only a current-voltage (J - V) characteristic and EQE spectrum, and thus it is possible to find the spectral efficiency of, e.g., the record cells in the *Solar cell efficiency tables*⁴.

Figure 2a displays the spectral efficiency of several record PV cells, and Figure 2b displays the limiting spectral efficiencies of cells with a range of bandgaps. Each spectral efficiency curve peaks near the absorber's bandgap wavelength; longer wavelengths are not absorbed and result in zero efficiency, and shorter wavelengths are converted with lower efficiency because of carrier thermalization. The utility of spectral efficiency in designing tandems is that cells of different technologies can be directly compared, and that the benefit of diverting photons from silicon to a candidate top cell is visually apparent. For example, Figure 2a reveals that, even though a-Si:H has the ideal bandgap for a top cell, the best a-Si:H cell converts every wavelength to electricity with poorer efficiency than the best monocrystalline silicon cell, and thus their tandem will necessarily have worse performance than the bottom cell alone. Conversely, GaInP, which has a similar bandgap to a-Si:H, can provide a substantial efficiency boost if coupled with silicon so that wavelengths shorter than 650 nm are absorbed in the GaInP cell.

Picking partners

The maximum efficiency of a tandem can be calculated by summing the integrated sub-cell spectral efficiencies, weighted by the spectra reaching each sub-cell, and then normalizing to the incident photon power:

$$\eta_{\text{tandem}} = \frac{\int \eta_{\text{top}}(\lambda) \cdot f_{\text{top}}(\lambda) \cdot I(\lambda) d\lambda + \int \eta_{\text{bottom}}(\lambda) \cdot f_{\text{bottom}}(\lambda) \cdot I(\lambda) d\lambda}{\int I(\lambda) d\lambda}, \quad (3)$$

$$\text{with } f_k(\lambda) = \frac{\Phi_k(\lambda)}{\Phi_{\text{incident}}(\lambda)} \quad (4)$$

the (wavelength-resolved) spectral fidelity—the fraction of the incident light with wavelength λ that reaches the k th cell (Φ is photon flux). The efficiency given by Equation 3 is that of *a tandem composed of two existing cells coupled losslessly*. This means no electrical losses (e.g., due to imperfect current matching), and thus implicitly assumes a four-terminal configuration, as well as no optical losses (e.g., due to parasitic absorption).

There are two common assumptions for the spectral fidelities. For a mechanically stacked tandem, $f_{\text{top}}(\lambda) = 1$ (all light reaches the top cell) and $f_{\text{bottom}}(\lambda) = T_{\text{top}}$ (all light transmitted through the top cell reaches the bottom cell). For two cells coupled with a beam splitter, $f_{\text{top}}(\lambda) = 1$ for λ shorter than $\lambda_{\text{top=bottom}}$ (the wavelength at which the top- and bottom-cell spectral efficiencies are equal) and 0 for longer

wavelengths, whereas $f_{bottom}(\lambda) = 0$ for λ shorter than $\lambda_{top=bottom}$ and 1 for longer wavelengths. That is, the beam splitter is perfect.

Figure 2c lists the maximum efficiencies of tandems made from the cells in Figure 2a using the $f_k(\lambda)$ values corresponding to the two coupling cases described above (mechanical stacking, beam splitter). One surprise is that the best perovskite cell on the best monocrystalline silicon cell results in only a marginal gain in efficiency (approximately 4% absolute) when the two sub-cells are coupled losslessly. As there will undoubtedly be at least optical losses in their coupling, it will be challenging to significantly exceed the efficiency of the silicon cell alone (25.6%) using present perovskites*. Note, however, that the best perovskite cell with the best multi-crystalline silicon cell reaches nearly as high an efficiency and offers a substantial boost compared to the inexpensive multi-crystalline silicon cell alone (21.3%). Another surprise is that, of all existing PV cells, GaAs would make the best top cell, even though it has the “wrong” bandgap according to Figure 1c. This is because it is much more efficient—that is, closer to its detailed-balance limit—than the other cells.

Tomorrow’s top cell

In evaluating new tandem possibilities, the best approach is to calculate the maximum tandem efficiency using the measured spectral efficiencies of the two cells of interest, as in Figure 2c. It is also possible, however, to construct a top-cell design guide using *approximate* spectral efficiencies calculated by derating the limiting spectral efficiencies shown in Figure 2b. Figure 3 is such a guide and predicts the efficiencies of tandems that pair a 20%- or 25%-efficient silicon bottom cell with top cells of varying bandgap and efficiency derating. The derating is expressed on the x-axis as the fraction of the detailed-balance efficiency, and the one-sun efficiencies of the top cells are also given by the gray contours.

Although Figure 3 is approximate, it successfully reproduces the exact results for existing sub-cells. For example, consider the GaInP cell in Figure 3b, which assumes a 25%-efficient silicon bottom cell that is similar to the 25.6%-efficient record cell in Figure 2c. The star, which was placed based on the InGaP cell’s bandgap and efficiency relative to the detailed-balance limit, corresponds to both the correct top-cell one-sun efficiency (slightly less than 21%, from the gray contour lines) and the tandem efficiency (slightly over 34%, from the color contours). This indicates how to use this guide to quickly evaluate

* An exception is if the sub-cells are coupled optically with an excellent beam splitter—see the 28.0%-efficiency tandem in Figure 1a—but this configuration is usually regarded as a laboratory demonstration that will not be manufactured.

candidate top cells: Find the cell's bandgap on the y-axis and its one-sun efficiency with the gray contours[†]. The color then indicates the maximum tandem efficiency possible if this cell were coupled with a 20%- or 25%-efficient silicon bottom cell.

Top-cell material		Bandgap	Efficiency	Year	Group/Institute	Coupling
III-V	AlGaAs	1.6 eV	25.2%	2012	Univ. of Tokyo ¹⁸	Two-terminal; fusion bonding
	AlGaAs	1.6 eV	21.2%	1998	Nagoya Inst. of Tech. ¹⁹	Two-terminal; epitaxial growth
	GaNP	1.8 eV	29.8%	2016	NREL ⁹	Four-terminal; mechanical stack
II-VI	CdZnTe	1.8 eV	16.8%	2010	EPIR Technologies ¹⁰	Two-terminal; epitaxial growth
Perovskite	CH ₃ NH ₃ PbI ₃	1.6 eV	19.2%	2016	EPFL et al. ¹²	Two-terminal; direct deposition
	CH ₃ NH ₃ PbI ₃	1.6 eV	22.8%	2015	EPFL et al. ²⁰	Four-terminal; mechanical stack
	CH ₃ NH ₃ PbI ₃	1.6 eV	28.0%	2015	Kaneka et al. ¹¹	Four-terminal; optical coupling
	CH ₃ NH ₃ PbBr ₃	2.3 eV	23.4%	2015	UNSW et al. ¹³	Four-terminal; optical coupling

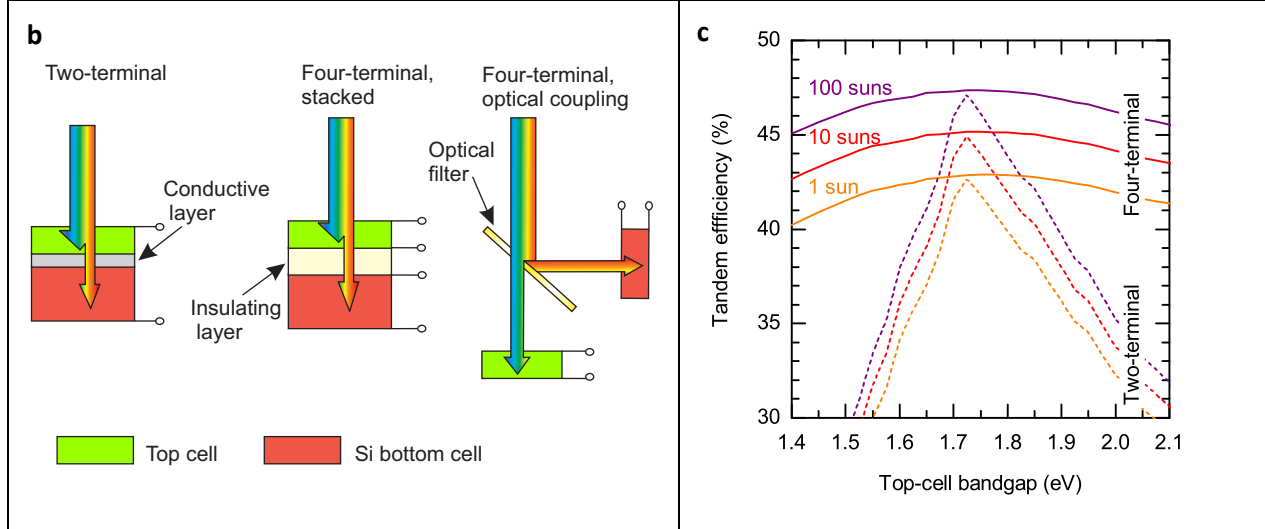
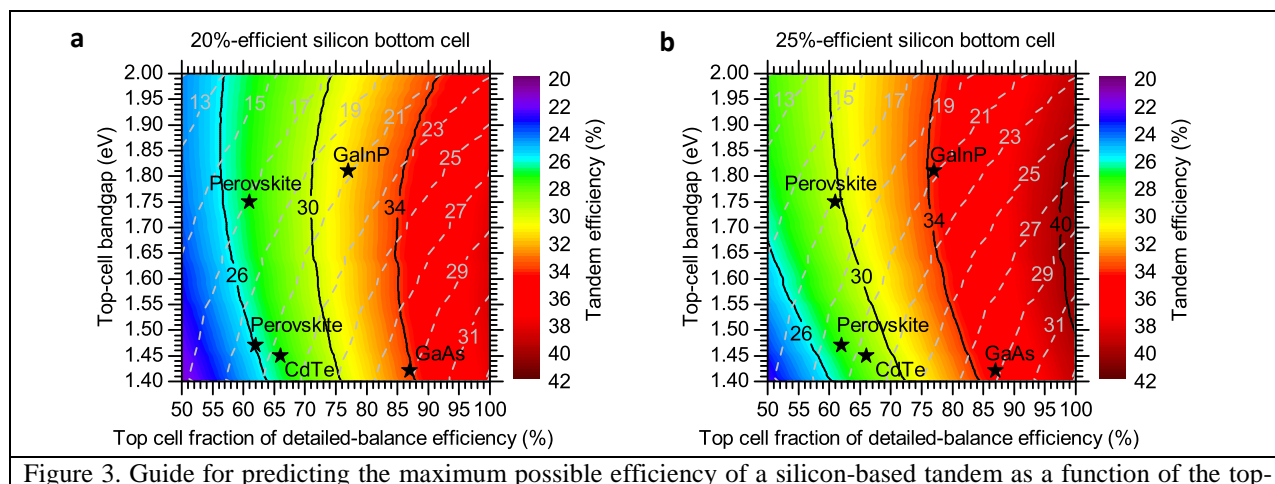
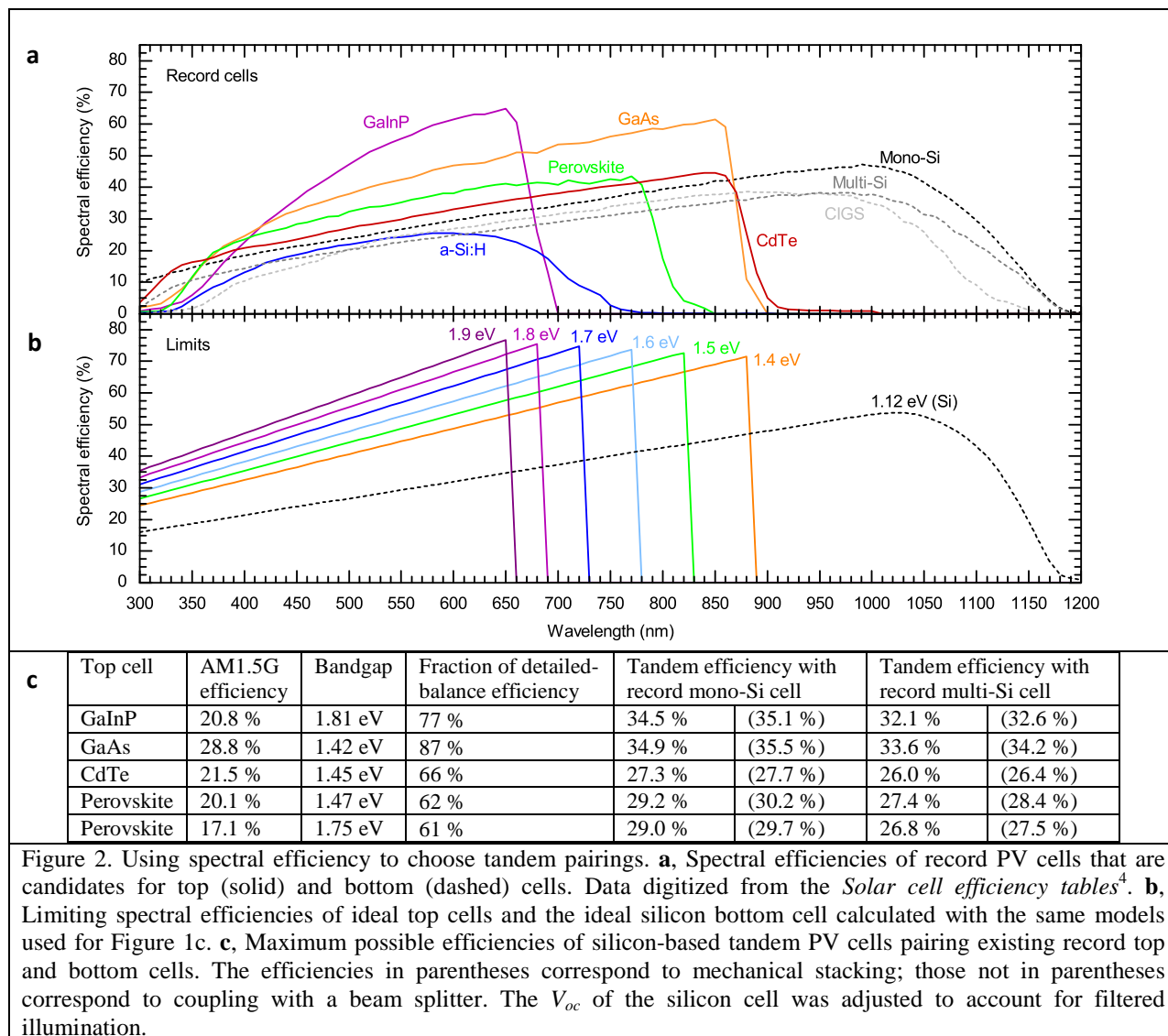


Figure 1. Present state of the art and limiting efficiencies for silicon-based tandem PV cells measured under AM1.5G (1000 W/m²) illumination. **a**, Record tandem efficiencies achieved for a range of top-cell materials and coupling configurations. **b**, Three common coupling configurations. **c**, Limiting efficiency of a silicon-based tandem PV cell for varying top-cell bandgap. Efficiencies are shown for two- and four-terminal configurations, as well as three illumination intensities. The efficiency of the silicon bottom cell was calculated with a model that includes Auger recombination and Lambertian light trapping⁵; the efficiency of the top cell was calculated with a detailed-balance model (radiative recombination only).

[†] This is usually easier than finding the fraction of the detailed-balance limit on the x-axis, but the result is the same.



cell bandgap and efficiency. **a**, Tandem with a silicon bottom cell that is 20% efficient when measured alone. **b**, Tandem with a silicon bottom cell that is 25% efficient when measured alone. In each plot, the color scale and black contour lines indicate the tandem efficiency, and the dashed grey contour lines indicate the efficiency of the top cell when measured alone. To obtain the approximate spectral efficiencies of the sub-cells used to calculate the tandem efficiency, the limiting spectral efficiencies in Figure 2b were derated by scaling them by a constant factor. According to Equation 1, this is equivalent to reducing the V_{oc} or FF of an ideal cell, or reducing its $J_{sc}(\lambda)$ by the same fraction at each wavelength.

- 1 Powell, D. M. *et al. Energy Environ. Sci.* **5**, 5874-5883 (2012).
- 2 Goodrich, A. C. *et al. Energy Environ. Sci.* **6**, 2811-2821 (2013).
- 3 Battaglia, C. *et al. Energy Environ. Sci.*, doi:10.1039/C5EE03380B (2016).
- 4 Green, M. A. *et al. Prog. Photovolt.* **24**, 3-11 (2016).
- 5 Richter, A. *et al. IEEE J. Photovolt.* **3**, 1184-1191 (2013).
- 6 Smith, D. D. *et al. IEEE J. Photovolt.* **4**, 1465-1469 (2014).
- 7 Green, M. A. *Nature Energy* **1**, 15015 (2016).
- 8 International Technology Roadmap for Photovoltaic (ITRPV): Results 2015. (2016).
- 9 Essig, S. *et al. IEEE J. Photovolt.* **accepted** (2016).
- 10 Garland, J. W. *et al. J. Appl. Phys.* **109**, 102423 (2011)
- 11 Uzu, H. *et al. Appl. Phys. Lett.* **106**, 013506 (2015).
- 12 Werner, J. *et al. J. Phys. Chem. Lett.* **7**, 161-166 (2016).
- 13 Sheng, R. *et al. J. Phys. Chem. Lett.* **6**, 3931-3934 (2015).
- 14 Liu, H. *et al. Opt. Express* **23**, A382-A390 (2015).
- 15 Kurtz, S. *et al. Prog Photovoltaics Res Appl* **16**, 537-546 (2008).
- 16 Russo, J. M. *et al. in Renewable Energy and the Environment.* RW1D.2 (Optical Society of America).
- 17 Yu, Z. J. *et al. IEEE J. Photovolt.* **5**, 1791-1799 (2015).
- 18 Tanabe, K. *et al. Sci. Rep.* **2** (2012).
- 19 Umeno, M. *et al. Sol. Energ. Mat. Sol. Cells* **50**, 203-212 (1998).
- 20 Werner, J. *et al. in European PV Solar Energy Conference and Exhibition, 31st* (Hamburg, 2015).